



1	Speciated Volatile Organic Compounds and Hydroxyl Radical Reactivity
2	Characteristics of Evaporation Emissions from China VI and China V In-use
3	Light Duty Gasoline Vehicles
4	Liuwei Kong ¹ , Xin Li ^{1,2,*} , Yu Wang ¹ , Sihua Lu ¹ , Ying Liu ¹ , Shengrong Lou ^{3,4} , Wenxin
5	Zhou ^{3,4} , Xinping Yang ^{5,6} , Yan Ding ^{5,6} , Yi Liu ¹ , Mengdi Song ¹ , Shuyu He ¹ , Kai Wang ⁷ ,
6	Feng Wang ⁷ , Xiaocen Shi ⁷ , Jian Wang ⁸ , Yun Zou ⁸ , Chaofan Lian ⁹ , Hefan Liu ¹⁰ , Miao
7	Feng ¹⁰ , Xiaoya Dou ¹¹ , Limin Zeng ¹ , Yuanhang Zhang ¹
8	¹ State Key Laboratory of Regional Environment and Sustainability, College of
9	Environmental Sciences and Engineering, Peking University, Beijing, 100871, P.R.
10	China
11	² Collaborative Innovation Center of Atmospheric Environment and Equipment
12	Technology, Nanjing University of Information Science & Technology, Nanjing,
13	210044, P.R. China
14	³ Key Laboratory of Formation and Prevention of Urban Air Pollution Complex,
15	Ministry of Ecology and Environment, Shanghai Academy of Environmental
16	Sciences, Shanghai 200233, China
17	⁴ School of Energy and Power Engineering, University of Shanghai for Science and
18	Technology, Shanghai 200093, China
19	⁵ State Environmental Protection Key Laboratory of Vehicle Emission Control and
20	Simulation, Chinese Research Academy of Environmental Sciences, Beijing,
21	100012, China
22	⁶ Vehicle Emission Control Center, Chinese Research Academy of Environmental
23	Sciences, Beijing, 100012, China
24	⁷ China Automotive Technology and Research Center, Beijing, 100176, China
25	⁸ Chengdu Vehicle Environmental Protection Technology Co., Ltd, Chengdu, 610000,
26	China
27	⁹ Tianfu Yongxing Laboratory, Chengdu 610213, China
28	¹⁰ Chengdu Academy of Environmental Sciences, Chengdu 610072, China
29	¹¹ College of Architecture and Environment, Sichuan University, Chengdu, 610065,
30	China
31	*: Corresponding Author: Xin Li; Email (li xin@pku.edu.cn)
32	ABSTRACT
00	7/1:1
33	Vehicle evaporation emission is one of the important sources of volatile organic
34	compounds (VOCs) in the atmosphere. Research on its emission factors and chemical
35	composition, especially the emissions from in-use vehicles under the new regulatory
36	standards, is still scarce and affects the understanding of evaporation emissions. In this
37	work, evaporative emission measurement for in-use gasoline vehicles was carried out

64

65

66





38 for the China VI and V vehicles, and their emission factors, chemical compositions and Hydroxyl radical total reactivity (koH) were measured. These three evaporative 39 emission processes, hot soak loss (HSL), diurnal breathing loss (DBL) 24h, and DBL 40 41 48h emission factors, China V vehicles can reach 3.2, 4.6 and 7.6 times that of China VI vehicles, and high mileage vehicle aging and abnormal evaporative emission control 42 systems can significantly increase emissions. In the HSL process, aromatics dominate, 43 with contributions from China VI and V reaching 44.1% and 42.8%, followed by light 44 carbon alkanes (LC-alkanes, \(\le C6 \)). In the DBL process, the chemical components were 45 dominated by LC-alkanes (40.7 - 50.5%). The source profiles analysis shown that n-46 butane (3.3 - 26.3%), iso-pentane (6.2 - 13.7%), toluene (6.1 - 16.2%) were the 47 dominant components. It was also discovered that n-pentane/ethane and methyl tert-48 butyl ether/benzene with can be used to discriminate the sources of evaporative 49 emissions and exhaust. The koH analysis revealed that branched chain alkenes (BC-50 51 alkenes), liner alkenes and aromatics were the most reactive components. It is necessary to strengthen the measurement of high reactivity alkenes, especially BC-alkenes, in 52 53 future research. 54 **Keywords:** Gasoline vehicles; Evaporative emissions; Source profiles; OH reactivity **Short summary:** Our research investigates the volatile organic compounds evaporative 55 56 emission characteristics of China's typical representative vehicle regulatory standards. 57 The emission factors, chemical composition characteristics and source profiles of volatile organic compounds were determined. The hydroxyl radical total reactivity and 58 compositions of evaporative emissions were quantified, and identified key volatile 59 60 organic compounds reactive species contributing to atmospheric photochemical processes. 61 1. Introduction 62

VOCs are precursors of ozone and secondary organic aerosols, and have significant impacts on air pollution and human health (Li et al., 2019; Guan et al., 2021). Gasoline vehicles are an important source of VOCs emissions which originate mainly from exhaust and evaporative emission processes (Song et al., 2018; Li et al., 2022; Liu et





67 al., 2017; Yan et al., 2021). In recent years, with the update of emission standards, the VOCs emissions from vehicle exhaust have decreased significantly, and the problem of 68 evaporative emissions has gradually become prominent. For example, in 2016, China's 69 70 vehicle evaporative emissions and exhaust emissions contributed 73% and 27% respectively (Yan et al., 2021). Meanwhile, for the vehicle emission factors, the current 71 evaporative emission factor is also significantly greater than the exhaust emission factor 72 73 (Liu et al., 2015; Zhu et al., 2017; Rodríguez et al., 2019). For example, for Euro 4 vehicles, evaporation emission and exhaust were 0.14 and 0.08 g/km respectively (Liu 74 et al., 2015). Therefore, evaporative emissions from vehicles have become an important 75 source of VOCs emissions from vehicles. The main processes of evaporative emissions 76 from vehicles are hot soak loss (HSL), diurnal breathing loss (DBL), and running loss 77 etc. (Liu et al., 2015). HSL refers to the emissions during the parking period of a vehicle 78 after driving for a period (one hour after turning off the engine); DBL refers to the 79 80 situation where the headspace pressure of the fuel tank changes due to temperature fluctuations between day and night, resulting in the emission of headspace vapor; 81 Running loss refers to the evaporative emissions during vehicle operation. 82 83 From the perspective of evaporative emission factors of vehicles in the fleet, E4 (European Union standards) vehicles are significantly higher than T2 (United States 84 85 standards) vehicles, for example, when DBL24 (emissions on the first day after parking), E4 and T2 were 0.834 and 0.297g/d, respectively. This difference is mainly 86 due to differences in the vehicle's evaporative emission control system, with significant 87 differences in control efficiency (Liu et al., 2015). For vehicles with Chinese standards, 88 89 China V vehicles (equivalent to E4) have an average emission of 0.88 g/d in the DBL24, which was also higher than the T2 (Zhu et al., 2022). Research on China VI shows that 90 DBL24 emissions are 0.25 g/d, significantly lower than the China V standard and close 91 to the emissions results of vehicles in the T2 (Zhu et al., 2022). China vehicle 92 evaporative emissions standard has significantly tightened its evaporative emissions 93 during the China VI standard stage (0.7 g/test) in 2020. The China VI standard has 94 significantly decreased compared to the previous standard (2 g/test). Currently, China 95





96 VI gasoline vehicles account for 9.9% of the total emissions of hydrocarbons in China (Ministry of Ecology and Environment, 2024), which implies that most vehicles in the 97 Chinese fleet are in a high emission state under the old regulatory standards. Moreover, 98 99 Gasoline vehicles account for 88.7% of the Chinese fleet, while diesel vehicles account for 41.3% in the European Union (Ministry of Ecology and Environment, 2019; 100 Chossiere et al., 2018). A higher proportion of gasoline vehicles in the fleet can lead to 101 higher evaporative emissions. Therefore, from the perspective of emission standards 102 and fleet fuel formula, China faces a more severe situation for evaporative emission 103 control compared to the United States and the European Union. 104 At present, offline sampling of SUMMA canister combined with GC-MS/FID (gas 105 chromatography-mass spectrometry/flame ionization detection) is commonly used for 106 measurement to obtain the chemical composition characteristics of evaporative 107 emissions. However, there are significant differences in understanding in different 108 109 studies. For example, some studies suggest that the proportion of alkanes in the DBL process reaches 68.5 - 82.6%, while others suggest it is 42.1 - 50.8%. This difference 110 was mainly due to the different number of species being focused on, with the former 111 112 testing 57 VOCs and the latter testing 108 VOCs (Yue et al., 2017; Liu et al., 2022b). In the emission process of different emission standards for vehicle models, there are 113 also significant differences in composition. Taking OVOCs as an example, the 114 115 proportion of vehicles in China VI and China IV/V were 33.1% and 14.1%, respectively(Zi et al., 2023). Moreover, in terms of emission factors, the DBL24 116 emissions of in-use vehicle and new vehicle in China V are 5.27 g/test and 0.81 g/test, 117 118 respectively, indicating that in use vehicles may have significantly increased emissions due to aging vehicle configurations (Liu et al., 2022b). However, previous study has 119 also suggested that the in-use vehicle of China V (DBL24) was 0.55 g/test (Yue et al., 120 2020). This significant difference in chemical composition and emission factors also 121 122 lead to inconsistent understanding of evaporative emissions. Therefore, further research is needed on the composition of chemical components and emission factors, especially 123 on the China VI vehicles after the revision of evaporative emission standards, which 124





are still relatively rare compared to vehicle research in China V and before.

In this work, we focus on the emission and chemical reactivity components 126 characteristics of VOCs evaporative emission from gasoline vehicles in-use by China 127 VI and China V vehicles. By utilizing a designed measurement system, and improving 128 VOCs measurement methods, the measurement of reactive species can be achieved. 129 Quantified and evaluated the emission factors and chemical composition of different 130 vehicle models and emission processes, established corresponding evaporative 131 emission source profiles, and identified the key reactive components of evaporative 132 emissions through OH radical reactivity analysis (Lou et al., 2010; Sha et al., 2022). 133 Improved the understanding of VOCs reactive species in the evaporative emissions of 134 China VI and China V vehicles, providing important reference for the emission control 135

2. Experiments and Methods

and management of vehicle emissions.

136

137138

139

140141

142143

144

145

146147

148

149

150

151

152

153

2.1. Vehicle testing procedures

The experiment takes light duty gasoline vehicles as the test objects, all of which are in-use, including a total of 9 vehicles, with 4 China VI vehicles and 5 China V vehicles. More common sedan and sport utility vehicles were chosen, while also considering compact and intermediate car, to reflect the actual composition characteristics of the Chinese fleet as much as possible (Table 1). The gasoline used in the experiment was China VI stage 95# gasoline, which was obtained through customization (The composition can refer to Table S1). Evaporative emissions test was carried out in the variable-temperature sealed housing for evaporative determination (SHED, AVL MAGNUM), which can achieve a constant temperature and simulate diurnal temperature changes, meeting the measurement requirements for evaporative emissions. To facilitate the comparison of emission differences among different vehicles, this study adopted a unified measurement method in the experiment. The pretreatment and testing procedures of the all vehicles in the experiment were based on the China VI stage emission standard method, this ensures the consistency and comparability of the experimental results (Figure S1a). In addition, we also conducted tests on the China V

155

156

157

158

159

160

161

162

163

164

165

166167

168

169170

171172

173

174

175176





method, which differs from the China VI method in terms of testing temperature and pre-treatment process, compare the differences in different testing methods for China V vehicles (Figure S1b). After the vehicle undergoes various processes, such as draining gasoline, refueling, pre-treatment driving, carbon canister loading, and hightemperature driving, HSL, DBL24 and DBL48 (emissions on the second day after parking) measurement are conducted in the SHED. In the carbon canister loading process, n-butane was used to load and test the carbon canister adsorption capacity (CCAC). The n-butane loading rate was set to 40 g/h, and the gas will first pass through the tested carbon canister. A second carbon canister was connected to the tested carbon canister outlet. When the mass of the second carbon canister increases by 2 g, it was considered that the tested carbon canister was fully loaded. At this point, the increase in mass of the tested carbon canister was the CCAC. During the experiment, the carbon canister of vehicle I was clogged due to aging issues during the loading process. After multiple attempts, until the breakdown value of n-butane reaches the breakthrough point of 2 g, the loading was completed. So, vehicle I did not obtain a loading amount that can reflect the actual CCAC. Vehicle G' was subjected to the China V testing method, in which the first step is to load the carbon canister. As the vehicle has just completed the China VI testing method process (parking time greater than two days), a portion of the gasoline vapor adsorbed in the canister does not have the actual CCAC loading amount, so this test does not focus on the CCAC value. For the HSL sampling schedule, sampling was performed at the beginning and end. DBL was sampled at 0h, 24h, and 48 h. A total of 11 experimental tests were carried out.

6





177 Table 1. Test vehicle information.

Stages	Model	Vehicles	Odometer(km)	Displacement(ml)	CCAC(g)	Tank(L)
	sedan	A	50033	1395	140.32	68.5
China VII	sedan	В	106245	1498	83.61	52.8
China VI	SUVs	C	50455	1984	134.64	60
	SUVs	D	155386	1499	73.32	58
	sedan	Е	87727	1598	33.28	55
	sedan	F	132237	1591	60.02	53
	SUVs	G	87036	1984	37.52	63
China V	SUVs	G'	87146	1984	*	63
	sedan	Н	89354	1984	12.58	64
	sedan	I	82489	1798	*	70
	sedan	I,	85271	1798	30.09	70

G': Using the China V evaporative emission testing method; I': replace the carbon canister of vehicle I; CCAC: Carbon canister adsorption capacity. *: The loading capacity of the carbon canister cannot be counted, please refer to section 2.1 for details.

178 2.2. Sample collection and analysis

To simultaneously characterize the chemical components and OH radical total reactivity (ko_H) characteristics of evaporative emissions, we designed an evaporative emission dilution sampling system. Total hydrocarbons (THC), VOCs, inorganic gases, and ko_H from evaporative emissions were measured. Figure 1 shows the conceptual diagram of the evaporative emission measurement system.





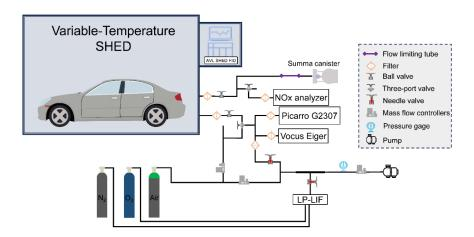


Figure 1. Conceptual diagram of evaporative emission sampling analysis system

The measurement of THC was carried out by equipment configured in the SHED, with equipment model AVL SHED FID I60 LH (unit is g). Calibration of the equipment was performed before and after each test. The concentrations of nitrogen oxides were also examined, using a commercial SAILHERO XHN200B instrument (with a sample flow rate of 0.5 L/min, the detection limit was 0.4 ppb) and a Thermo Fisher Scientific Model 42i Trace Level instrument (sample flow rate of 1 L/min, the detection limit was 0.05 ppb). A commercial instrument by Cavity Ring-Down Spectroscopy method (Picarro G2307) was used to measure formaldehyde, and the sampling flow rate was approximately 0.4 L/min, and the detection limit was 0.16 ppb (1σ).

A proton transfer reaction time-of-flight mass spectrometry (VOCUS-Eiger, ToFWerk) was used for real-time measurement of OVOCs components (sampling flow rate of approximately 0.08 L/min). During the experiment, standard gas was injected every day to compare the changes in the sensitivity of the equipment and evaluate the working state of the equipment (e.g. m-xylene was approximately 1000 cps/ppb). Tofware v3.2.3 was used for mass spectrometry peak identification and fitting. Six OVOCs were used for quantification (Table S2).

The main VOCs components of evaporative emissions were sampled using silicalined SUMMA canisters, and following using GC-MS/FID for quantitative analysis. To prevent errors caused by the instantaneous sampling of the SUMMA canisters, a flow





limiting tube was used to stabilize the sampling flow. The collected offline samples (SUMMA canisters) were undergoing pressure dilution pretreatment before the GC-206 MS/FID analysis. During the experiment sample analysis, the equipment was regularly 207 208 calibrated, and the calibration curve was updated. The detection limit for species was between 5 - 50 ppt. The VOCs species were shown in Table S3 (supplementary 209 materials). In the experiment, the calibration equipment was performed, and mixed 210 standard gases and 7 branched chain alkene standard gases were used to obtain 211 quantitative calibration curves (supplementary materials Text S1 and Table S4). 212 The k_{OH} refers to the comprehensive ability of OH radicals in the atmosphere to react 213 with reactive gas components, which can be directly measured and calculated based on 214 the reactive gas components(Kovacs and Brune, 2001; Yang et al., 2019). Direct 215 measurement of the OH radicals total reactivity (k_{OH}^{mea}) was carried out using the laser 216 photolysis laser-induced fluorescence (LP-LIF) device deployed by Lou et al.(2010), 217 218 which has been applied in field observations and vehicle source emissions(Lou et al., 2010; Liu et al., 2023; Sha et al., 2022; Liu et al., 2019). A detailed description of the 219 220 LP-LIF equipment details was provided in the supplementary materials (Text S2 and 221 Figure S2). Considering the working flow rate and measurement range of LP-LIF, the allowed sampling volume of SHED and the koH range of evaporative emissions are not 222 223 suitable for the normal operation of LP-LIF. A dilution sampling system was designed 224 to measure the evaporative emissions k_{OH} (Figure 1). The k_{OH} measurement was divided into two stages of dilution. The first stage was achieved by suppling 3 L/min of 225 synthetic air and mixing it with approximately 1 L/min of sampling in a mixing tube. 226 227 The second stage involves LP-LIF sampling approximately 1 L/min of gas from the mixing tube and mixing it with 12 L/min of the gas supplied by the LP-LIF system to 228 achieve second stage dilution. By adjusting and measuring the primary and secondary 229 sampling flow rates during the experiment, specific dilution coefficients can be 230 231 obtained to achieve the measurement of koh. By conducting zero gas (background testing) testing on LP-LIF and repeating it 7 times, the method detection limit of LP-232 LIF was 0.6 s⁻¹ (3σ). The variation characteristics were tested within 50 s⁻¹, which 233





- 234 revealed linear changes that met the measurement requirements of this experiment.
- 235 Considering the combination of the dilution sampling system and the LP-LIF
- 236 measurement system, and through standard gas testing, comparing reactivity
- 237 measurement and calculation, the error of this measurement system estimated at
- 238 approximately 15%. To increase the number of samples and reduce measurement errors,
- 239 resulting in a total sampling time of about 8 minutes. This time setting considers both
- 240 the impact of sampling volume on the normal operation of SHED and the reliability of
- 241 equipment testing results.

2.42 2.3. Calculation of evaporated emission species mass

243 The VOCs evaporation compositions mass was given by:

$$EF_{i} = \frac{(C_{i,end} - C_{i,start}) \times V_{s} \times P \times M_{i}}{R \times T \times 10^{9}}$$
(1)

- 245 where EF_i is the evaporative emission mass of species i, g; C_{i,end} is the final
- 246 concentration of species i within SHED, ppb; C_{i,start} is the initial concentration of
- species i within SHED, ppb; V_s is the corrected volume of SHED, m³; P is the average
- 248 pressure at the start and end of the sampling process, Pa; M_i is the molar mass of species
- 249 i, g/mol; R is the gas constant, 8.314 J/mol/K; and T is the average temperature at the
- 250 start and end of the sampling process, K. In the evaporative emission process, the unit
- of HSL is g/h, and, the unit of DBL is g/d.

252

2.4. Calculation of the OH total reactivity

- The calculation of k_{OH}^{cal} is based on the sum of the measured concentration of the
- 254 reactive gas multiplied by the corresponding rate constant of the OH radical reaction.
- 255 The expression can be expressed as in Equation (2).

256
$$k_{OH}^{cal} = \sum k_i \times [Reactive gas_i]$$
 (2)

- 257 where Reactive gasi (molecule/cm³) is the measured concentration of organic and
- 258 inorganic gases in this experiment. k_i (cm³/molecule/s) is the reaction rate constant of
- 259 the OH radicals corresponding to the reactive gases. k obtained from NIST Chemical
- 260 Kinetics Database, Master Chemical Mechanism (v3.3.1), and International Union of
- 261 Pure and Applied Chemistry (IUPAC) databases. For detailed data on the parameter ki,
- please refer to Table S5.

264





3. Results and discussion

3.1. Emission factors of THC

Figure 2 presents the measurement results for the evaporative emissions of THC 265 together with the relevant literature research results. The THC emissions of the China 266 VI vehicles are significantly lower than those of the China V vehicles. The THC values 267 of China V vehicles during HSL, DBL24 and DBL48 were 0.205 g/h, 0.599 g/d, and 268 0.904 g/d, respectively. The corresponding values for the China VI vehicles were 0.065 269 g/h, 0.132 g/d, and 0.119 g/d, respectively. Thus, the China V values are significantly 270 higher than the China VI values, with the HSL, DBL24 and DBL48 values 3.2, 4.6 and 271 7.6 times higher, respectively. The difference can be explained by the working ability 272 of the carbon canister. The carbon canister configured in China VI vehicles has a higher 273 CCAC compared to China V vehicles, with 119.5 g and 34.5 g respectively. The larger 274 CCAC reduces the volatile emissions of gasoline vapor from the fuel tank. The 275 276 evaporative emission limit of Chinese VI standard, which was fully implemented in 2020, is 0.7 g/test, which is close to the evaporative emission limit of 0.65 g/test in the 277 278 T2 stage of the United States. Through literature testing data, it can also reflect the 279 current emission control level of China VI vehicles. The T2 data in Figure 2 summarizes the research results of the literature, with HSL, DBL24, and DBL48 values of 0.052 280 281 g/h, 0.234 g/d, and 0.208 g/d, respectively(Liu et al., 2015; Man et al., 2018). Both 282 China VI and T2 emissions can meet the emission limit requirements, but from the DBL processes, the emission level of China VI was slightly lower than that of T2. A study 283 found that the DBL24 and DBL48 test results for China VI were 0.16 g/d and 0.198 g/d, 284 285 slightly higher than the results for China VI in this study. Comparing the CCAC of the vehicles, the CACC of the literature research vehicle was 81.04 g, which is lower than 286 that of the vehicle in this study (Zi et al., 2023). For both the China V vehicle and 287 literature study, the China VI measurement method was used, and it was found that the 288 289 DBL results were basically consistent within the fluctuation range. At the same time, it was also found that the carbon canister CCAC (15.45 g and 40.35 g) used in this study 290 was basically consistent (Zi et al., 2023). Therefore, from this comparison, it can also 291





be found that the working capacity of carbon canister has an impact on evaporative emissions. However, for the HSL process with lower emissions, there are slight differences, such as the results of China V, which are slightly higher in this study than in literature research. For example, the results of China V are slightly higher than the literature research's 0.104 g/h (Zi et al., 2023). This subtle difference may be due to differences in experimental vehicles, mileage, and gasoline, or it may be within the normal error range. More experiments will be needed in the future to verify this.

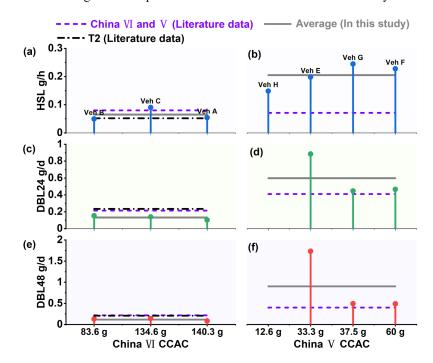


Figure 2. Evaporative emission factors of different vehicles and processes (Liu et al., 2015; Man et al., 2018; Zi et al., 2023). (a) China VI HSL; (b) China V HSL; (c) China VI DBL24; (d) China V DBL24; (e) China VI DBL48; (f) China V DBL48. CCAC: Carbon canister adsorption capacity. Vehicle information can be found in Table 1.

If the control system (carbon canister) malfunctions, emissions increase significantly. For example, in vehicle I (China V), there was an abnormal carbon canister, resulting in a significant decrease in the adsorption efficiency. In DBL24 and DBL48, the THC

309

310311

312

313

314

315

316

317

318

319

320 321

322323

324

325

326327

328

329330

331

332

333334

335

336





reached 1.987 g/d and 11.209 g/d, which was significantly higher than those of other China V vehicles (Figure S3). For the sake of comparison, we have replaced the carbon canister of vehicle I with an equivalent model. The results (I', China V) after the carbon canister were replaced were 0.345 g/d and 0.326 g/d, respectively. Comparing the results of I and I', abnormal malfunctions of the carbon canister will significantly affect the evaporative emissions (Figure S3). Compared with HSL, abnormal carbon canister has a greater impact on DBL emissions, which may be mainly due to the increased workload of the carbon canister caused by the headspace vapor of the fuel tank in response to temperature changes (20 - 35 °C), resulting in higher emissions from DBL. In addition, Higher ambient temperatures promote evaporative emissions (Huang et al., 2022). Using vehicle G (China VI test method) for testing, the THC of HSL was 1.5 times higher than the corresponding G' (China V test method) values (Figure S4). The testing procedure of China V has a temperature setting of 23 °C - 31 °C (test setting at 25 °C) in the HSL, which may not reflect the actual environmental conditions. By contrast, the 38 °C set by China VI HSL is closer to the environmental characteristics of the summer high temperature weather. For example, in Chengdu from August 7th to 24th, 2022, the daily maximum temperature ranges from 36.1 - 41.6 °C (Lei et al., 2024). Study has confirmed that when the temperature increases from 25 °C to 35 °C, the anthropogenic source VOCs concentration can increase by about 2 times (Qin et al., 2025). This also reflects the importance of testing evaporative emissions at high temperatures. In the DBL comparison, the China V test method was 14.4% higher than the China VI test method (Figure S4). The main reason for this difference may be due to the difference in the soak temperature setting during preprocessing. In China V, the requirement is 20-30 °C, while in China VI, it is 38 °C (Figure S1). A higher soak temperature is beneficial for the volatilization of pollutants. Therefore, in the DBL process, so there is a situation in the DBL process where the testing method in China VI was lower than that in China V. Previous studies have shown that the THC of China V new vehicles have emissions of 0.81 g/d for DBL24 (Liu et al., 2022b). For the DBL of China V in-use vehicles, the

338

339340

341

342

343

344

345

346

347

348

349350

351 352

353

354 355

356

357

358 359

360

361

362

363

364

365





results of this study were higher than those of new vehicles, and the emissions of China V in-use vehicles were 5.27 g/d for DBL24; This may be due to the high vehicle mileage, which causes aging and increases VOCs emissions, the mileage range of the new car were 2987 - 3065 km, and the in-use cars were 32012 and 36854 km (Liu et al., 2022b). However, high mileage vehicles may also be due to the reduced efficiency of the evaporative emission control system, resulting in higher evaporative emission results. In this experiment, we also found that the THC values of DBL24 and DBL48 from vehicle D, which was a China VI vehicle, were 0.55 g/d and 0.463 g/d (Figure S5), respectively, significantly higher (by approximately a factor of 4) than the average levels of other the China VI test vehicles. But the difference in HSL emissions is not significant (approximately 5.1%). The mileage of vehicle D was 1.6×10⁵ km, which is approximately 2.3 times higher than the average mileage (6.9×10⁴ km) of the other China VI test vehicles. We found that the CCAC of vehicle D was 73.32 g, which was lower than the average 83.61 -140.32 g of other vehicles. Due to the significant temperature changes (20 - 35 °C) during the DBL process, the fuel tank undergoes a breathing process through the carbon canister. The lower adsorption capacity of the carbon canister can lead to a decrease in control efficiency. This indicates that higher mileage may also significantly degrade the operational capability of the evaporative emission control system. In the future, it is necessary to establish a quantitative relationship between evaporative emissions and carbon canister efficiency for high mileage vehicles, which will help further analyze the influence of this high mileage vehicle aging factor.

3.2. Evaporative emission chemical compositions and source profiles

Figure 3 shows the chemical composition results of the VOCs evaporation emissions from the China VI and China V vehicles. LC-alkanes (≤C6, light carbon alkanes), aromatics and OVOCs were the main emission components. Compared with the DBL, the HSL has higher aromatics emission, whereas LC-alkanes contribute the most to the DBL. In the HSL process, the aromatics, LC-alkanes and OVOCs contents in China VI vehicles (A, B and C) were 44.1%, 22.2% and 18.6%, respectively, while those in China





366 V vehicles (E, F, G and H) were 42.8%, 26.6% and 10.1%, respectively. For DBL24, the aromatics, LC-alkanes and OVOCs contents in China VI vehicles (A, B and C) were 367 20.2%, 40.7% and 19.1%, respectively, while those in China V vehicles (E, F and G) 368 369 were 20.9%, 42.9% and 9.7%, respectively. For DBL48, the aromatics, LC-alkanes and OVOCs contents in China VI vehicles (A, B and C) were 14.3%, 45.8% and 17.6%, 370 respectively, while those in China V vehicles (E, F and G) were 15.3%, 50.5% and 8.5%, 371 respectively. There is also a significant difference in the proportion of OVOCs between 372 China V and China VI vehicles, contribution of OVOCs in China VI vehicles was 373 greater than that in China V; This situation will be further analyzed from the emission 374 source profiles in the following text. For L-alkenes (liner alkenes) and BC-alkenes 375 (alkenes with branched structures), China V vehicles showed higher values than China 376 VI vehicles, DBL values were higher than HSL values, and DBL48 values were higher 377 than DBL24 values. Overall, the proportion of L-alkenes (4 - 10.9%) was slightly 378 higher than that of BC-alkenes (2.7 - 7.8%). In addition, different measurement 379 methods were used for the China V vehicle, with vehicle G using the China VI 380 measurement method and G' using the China V measurement method, HSL and DBL24 381 382 were tested, and the chemical composition and proportion were basically the same. 383

15





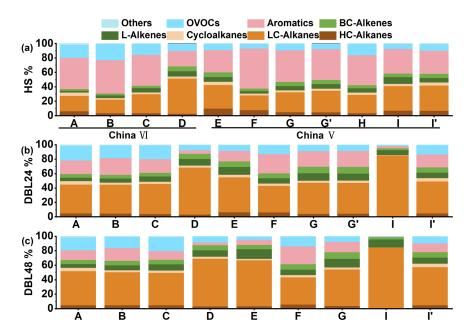


Figure 3. Composition characteristics of VOCs evaporation emissions from different vehicles. (a) HSL; (b) DBL24; (c) DBL48. Vehicle information can be found in Table 1.

The vehicle with higher emissions of THC were accompanied by a higher proportion of LC-alkanes (HSL, DBL24 and DBL48 were 48.8%, 65.4% and 65.8%, respectively), such as in the case of vehicle D (China VI high mileage). Meanwhile, in DBL24 and DBL48 of vehicle I (China V), the high emissions caused by abnormal carbon canister accounted for 84.2% of LC-alkanes, far higher than the average level of the China V vehicles. After replacing the carbon canister in Vehicle I (the result is denoted as I'), a significant decrease in emissions was observed, and the composition was also essentially the same as that for the other China V vehicles. In a previous study, Liu et al. focused on PAMS (Photo Assessment Monitoring Stations) and TO15 (Toxic Organics-15) species, and quantified the number of 108 VOCs species (Liu et al., 2022b). In this study, we quantitatively added 7 additional BC-alkenes and found that there was significant high reactivity BC-alkenes species in China V and China VI vehicles, and their contribution levels were also close to those of L-alkenes. By contrast, if only the PAMS component was considered, the proportion of alkanes will be





402 overestimated and the contribution of OVOCs will be ignored, for example, in the DBL24 process, alkanes proportion can reach 68.5 - 82.6% (Yue et al., 2017). The 403 contribution of BC-alkenes was comparable to that of L-alkenes, indicating the need to 404 405 include BC-alkenes in future vehicle emission tests to achieve the most comprehensive assessment of pollutants possible. A study on refueling emission and headspace vapor 406 testing found that alkanes dominate, accounting for 70.54% and 66%, the contribution 407 of aromatics was only 1.43% and 1.13%, respectively (Man et al., 2020). Comparing 408 the evaporative emission process, the DBL process of normal vehicles was lower than 409 this proportion, but for high emission vehicles, it was close to this proportion. But for 410 aromatics, evaporative emissions (14.3 - 44.1%) were significantly higher than the 411 proportion of refueling emission and headspace vapor. Aromatics and alkanes have 412 relatively high contributions in gasoline vehicle exhaust emission, accounting for 43.2% 413 and 32.3% respectively (Liu et al., 2024). Among them, the contribution of aromatics 414 415 was close to that of the HSL process in evaporative emissions, but the difference from the DBL process was obvious. Aromatics in DBL are not the largest contributing VOCs 416 component. And the exhaust emissions also have a high characteristic of alkynes 417 418 (9.57%) emissions, with alkynes being extremely low in evaporative emissions (Liu et al., 2024). 419 420 The measurement results of the evaporative emission source profiles for the China 421 VI and China V vehicles were shown in Figure 4. The source profiles calculation accounted for both normal and high-emission vehicle scenarios, and emission source 422 profiles were obtained for different emission processes. Sixty-three VOC species were 423 424 selected, including 8 HC-alkanes (high carbon alkanes, the number of carbon atoms >C6), 10 LC-alkanes, 4 cycloalkanes (alkanes with cyclic structures), 9 L-425 alkenes, 5 BC-alkenes, 15 aromatics and 12 OVOCs, accounting for more than 95% of 426 the total VOCs mass. Overall, n-butane (3.2 - 26.1%), iso-pentane (6.2 - 13.5%), n-427 pentane (3.6 - 8.4%), toluene (6.1 - 16.0%), m/p-xylene (2.5 - 10.7%), methyl tert-butyl 428 ether (MTBE) (5.3 - 7.4%) and 4-methyl-2-pentanone (0.4 - 5.8%) were the main 429 contributors. Compared with that during the HSL process, the proportion of n-butane 430

432

433

434

435

436

437

438

439

440

441

442

443 444

445

446447

448

449

450

451

452 453





during the DBL process significantly increases, whereas the proportions of toluene and m/p-xylene decrease. During each emission process, OVOCs were significantly higher in the China VI vehicles than in the China V vehicles, which was due mainly to species such as 4-methyl-2-pentanone and MTBE. The proportions of 4-methyl-2-pentanone in China VI and China V were 2.2 - 5.8% and 0.4 - 0.9%, respectively, with the corresponding MTBE values of 5.5 - 7.4% and 5.3 - 7.1%. From the DBL24 process to the DBL48 process, the proportion of n-butane in the China V vehicles increased significantly compared with that in the China VI vehicles. In the emission profiles of gasoline headspace, iso-pentane was the main component, and aromatics were not significant (Wu et al., 2015). If headspace is used to calculate the evaporative emissions of vehicles, significant uncertainty will be introduced. For BC-alkenes and L-alkenes, 2-methyl-2-butene (1.6 - 4.3%), 2-methyl-1-butene (0.7 - 2%), and trans-2-pentene (1.6 - 3.4%) were found to be the main components. Lu et al. tested the source profiles of BC-alkenes in gasoline vapor (Lu et al., 2003). Wang et al. reported that the contribution of BC-alkenes in headspace vapor was approximately 6.2% (Zhang et al., 2013). Liu et al. also observed the emission of BC-alkenes in the 2005 evaporative emission test (Liu et al., 2008). The research on BC-alkenes related to vehicle emissions sources is relatively early. Therefore, the addition of 2-methyl-2-butene and 2-methyl-1-butene also improved the previous evaporative emission profiles of China V and China VI vehicles (Liu et al., 2022b; Li et al., 2024; Zi et al., 2023). In addition, formaldehyde was an important emission characteristic of China VI vehicles, particularly in the HSL, with emissions reaching 1.6%, which is much higher than those of DBL and China V vehicles, and this result is consistent with the OVOCs results in Figure 3.





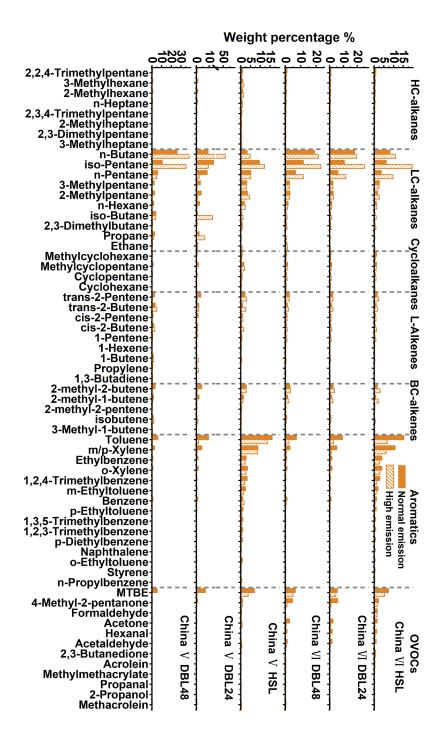


Figure 4. Weight percentage of HSL, DBL24 and DBL48 source profiles for evaporative emissions.





456 Figure 4 also compares the source profiles of high emission vehicles, such as China VI vehicles with high mileage features and China V vehicles with abnormal carbon 457 canister. Compared with normal China VI vehicle emissions, n-butane, iso-pentane, and 458 n-pentane of China VI have a significant increase. For example, for high emission 459 vehicles in China VI, n-butane, iso-pentane, and n-pentane were 11.0 - 21.3%, 19.5 -460 25.1%, and 9.7 - 11.8%, respectively. For high emission China V vehicles, carbon 461 canister breakthrough emissions were observed at DBL48, with n-butane and iso-462 pentane reaching 38.5% and 35.2%, far higher than the normal China V vehicle 463 emissions of 26.1% and 10.6%, respectively. For aromatics and OVOCs species, under 464 high emission conditions, the contribution of major species such as toluene, m/p-xylene, 465 and MTBE in the source profiles will decrease compared to normal vehicles. Overall, 466 due to vehicle anomalies such as aging at high mileage and abnormal carbon canister, 467 resulting in high evaporative emissions, the proportion of tracer species in the source 468 469 profile will increase compared to normal emission vehicles. 470 The species composition of evaporative emissions is characterized by relatively high proportion of n-butane (3.2 - 26.1%) and iso-pentane (6.2 - 13.5%), significantly 471 472 exceeding the proportion of ethane (0.03 - 1.0%). In contrast, in the exhaust emissions of gasoline vehicles, the contribution of ethane was comparable to or even exceeds that 473 of n-butane and iso-pentane; For example, in China V gasoline vehicles, ethane, n-474 butane, and iso-pentane were approximately 2.3%, 3.5%, and 2.0%, respectively; In 475 China VI gasoline vehicles, they correspond to approximately 6.5%, 0.8%, and 0.7%, 476 respectively (Li et al., 2024). This also reflects the VOCs species differences in 477 478 evaporative emissions and exhaust emissions. From the analysis of the ratio of characteristic species n-pentane to ethane, the exhaust ratios of China V and China VI 479 are approximately 1.1 and 0.6 (Li et al., 2024), respectively, corresponding to 6.5 -480 121.2 and 9.2 - 174.3 in evaporative emissions. It was also found that the ratio (n-481 pentane/ethane) of HSL was significantly higher than that of DBL. Additionally, the 482 MTBE/benzene (MTBE/B) ratio of HSL and DBL process ranged from 5.7 - 6.5. This 483 ratio is significantly higher in evaporative emissions than in exhaust related emission 484





485 sources, such as 1.07 and 0.6 in tunnels (Sun et al., 2019; Liu et al., 2022a), 1.3 in underground parking (Chai et al., 2023), 0.4 in diesel exhaust (Huang et al., 2020). 486 There are significant differences between evaporative emission sources and process and 487 solvent usage sources in terms of tracer species. There are usually high levels of 488 OVOCs species such as acetone, ethyl acetate, and n-butyl acetate in the process and 489 solvent sources, but the evaporative emissions have obvious MTBE and 4-methyl-2-490 pentanone emission characteristics, which can be used to identify evaporative 491 emissions (Zhao et al., 2018; Wang et al., 2017). Therefore, the above species 492 parameters can be used as important references for identifying vehicle evaporative 493 emissions. 494

3.3. OH reactivity characteristics

495

The direct measurement results of koH (koH (koH) for China VI and China V vehicles 496 were shown in Figure 5. Overall, the komea level of the China VI vehicles was 497 significantly lower than that of the China V vehicles. The k_{OH} values of China VI 498 vehicles (B and C) were 34.6 s⁻¹ and 72.2 s⁻¹, 157.4 s⁻¹ and 174.3 s⁻¹, 160.9 s⁻¹ and 194.7 499 s⁻¹ for HSL, DBL24 and DBL48, and the corresponding values for the China V vehicles 500 (E and G) were 213.4 s^{-1} and 278.7 s^{-1} , 1389.5 s^{-1} and 690 s^{-1} , 2851.9 s^{-1} and 805.3 s^{-1} , 501 respectively. The k_{OH}^{mea} values of HSL, DBL24 and DBL48 of vehicle D were 107.3 s⁻ 502 ¹, 708.9 s⁻¹ and 609.4 s⁻¹, respectively, which are significantly higher than those of China 503 504 VI vehicles (B and C), approaching the level of China V vehicles. This indicates that high mileage vehicles may have higher evaporative emission characteristics due to 505 evaporative emission control systems and vehicle aging. 506





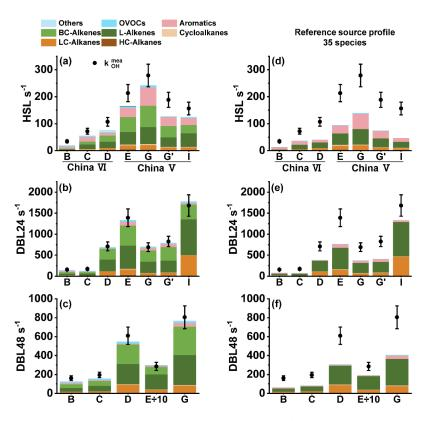


Figure 5. Comparative analysis of calculation (k_{OH}^{cal}) and direct measurement (k_{OH}^{mea}) of total OH reactivity. (a) HSL; (b) DBL24; (c) DBL48. Figure d, e and f shows the HSL, DBL24 and DBL48 reactivity closure calculation using species provided by literature source profiles (Liu et al., 2022b). Vehicle information can be found in Table 1.

Figure 5a, b, c and Figure 6 shows the composition proportion characteristics of the koh components calculated based on VOCs component measurements. There is a significant difference in the composition of the components compared to the results presented in Figure 3, L-alkenes, BC-alkenes and aromatics dominate the koh. In the reactive composition of the HSL process, L-alkenes account for 18.3 - 30.4%, BC-alkenes account for 14.8 - 33.4%, and aromatics contribute 20.9 - 39.8%. The contribution of L-alkenes and BC-alkenes to the reactivity in the DBL process occupies an absolute dominant position. During the DBL24 process, L-alkenes account for 26.6

522

523524

525

526527

528529

530

531

532

533534

535

536537

538539

540

541542

543

544

545

546547

548

549





the DBL48 process, the proportions of these three components were 30.9 - 54.9%, 26.7 - 39% and 3 - 11.3%, respectively. In the composition of chemical components, LCalkanes was relatively important contributors, especially in the DBL process, occupying a dominant position. However, in the composition of koH, the proportion of LC-alkanes in the DBL process was only 8.8 - 12%. This indicates that in VOCs emission reduction and control, priority can be given to L-alkenes and BC-alkenes with significant reactivity impact, thereby improving the effectiveness of atmospheric VOCs emission reduction and control. In the VOCs total emission reduction control strategy, considering the characteristics of emission sources and incorporating considerations based on reactive species is beneficial for achieving significant environmental benefits (Zhong et al., 2021; Wang et al., 2024). For vehicles with abnormally high VOCs emissions, such as high mileage China VI vehicle (vehicle D) and the China V vehicle with the abnormal carbon canister (vehicle I), the contribution of L-alkenes and BC-alkenes significantly increased and dominated, particularly during DBL24 and DBL48, where vehicle D (China VI) contributed 76.4% and 76.6%, respectively, and vehicle I (China V) contributed 67.2% and 77.7%. This indicates that vehicles with higher evaporative emission characteristics have significantly increased contributions to reactivity from L-alkenes and BC-alkenes in their reactivity component composition compared to normal emission vehicles. Based on the abnormal situation of the carbon canister in vehicle I, after replacing the canister, it was measured that in DBL48, the reactive components of L-alkenes, BC-alkenes, LCalkanes, OVOCs and aromatics were 35%, 35.5%, 11.9%, 6.6%, and 6%, respectively; However, under the abnormal situation of the carbon canister, they were 61.6%, 16.1%, 21.3%, 0.5% and 0.3%, respectively. It can be observed that the proportion of L-alkenes in vehicle I with abnormal carbon canister has significantly increased (61.6%). For the reactive composition of another high mileage emission vehicle D (with contributions of 30.7% and 29.7% for L-alkenes and BC-alkenes, respectively), it was found that there would be differences between the two emission mechanisms. When the vehicle

- 41.2%, BC-alkenes account for 25.7 - 38.2%, and aromatics contribute 6.8 - 16%; In





was in high mileage use, aging brings high emissions, and the carbon canister working system is in normal condition, species with branched structures will be more conducive to emissions, so the contribution of BC-alkenes in vehicle D has increased compared to vehicle B and vehicle C. On the contrary, when the carbon canister system was abnormal, gasoline vapor was emission directly, and low-carbon L-alkenes ware more conducive to emissions, resulting in a higher reactivity proportion of L-alkenes; For example, comparing the changes in DBL48 L-alkenes and BC-alkenes before and after replacing the carbon canister in vehicle I, the average number of L-alkene species increased by 71.9 times, while the average number of BC-alkenes increased by only 30.3 times, corresponding to an average of 4.2 (2 - 6) and 5.3 (4 - 6) carbon atoms, respectively.

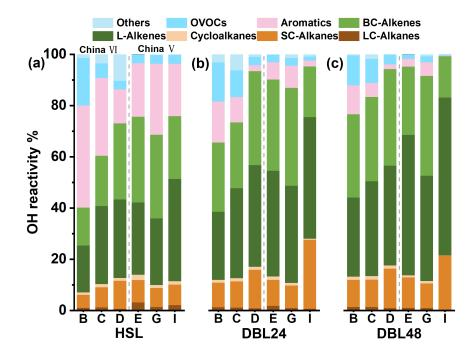


Figure 6. Contribution characteristics of the OH reactivity Calculation results of the evaporation emission components. (a) HSL; (b) DBL24; (c) DBL48. Vehicle information can be found in Table 1.

The k_{OH} can be determined through both k_{OH} and k_{OH} approaches. In theory, if

567

568

569

570

571

572

573

574

575

576

577

578

579

580

581 582

583 584

585

586587

588

589

590

591592

593

594





all reactive components are quantified, k_{OH}^{mea} should equal k_{OH}^{cal} . However, in practice, current analytical techniques cannot fully capture all chemical species in the measurement. By comparing k_{OH}^{mea} and k_{OH}^{cal} (a method referred to as OH reactivity closure analysis) the completeness of the observed chemical composition contributing to koh can be assessed. If koh is significantly lower than koh, it suggests the presence of unmeasured reactive species (OH reactivity missing source). From the perspective of OH reactivity closure, there is a significant missing reactivity in the HSL process compared with the DBL process, and the OH missing reactivity of the China VI vehicles was more pronounced (Figure 5a, b and c). The missing reactivity values of the HSL process for the China VI and China V vehicles were 31.2% (22.0 - 43.1%) and 18.5% (12.8 - 22.9%), respectively. Considering a measurement error of 15%, The HSL of China VI vehicles has missing reactivity, and some vehicles of China V vehicles have missing reactivity, such as vehicle E (22.9%) and vehicle I (20%). In the DBL process, the China V vehicles essentially demonstrated closure (-6.4 - 4.5%). By contrast, koH missing vehicles were found among the China VI vehicles, for example, missed reactivity of DBL24 for vehicle C was 22.8%, and the missed reactivity values for DBL48 of vehicle B and C was 21.6% and 19.4%, respectively. Overall, the tightening of evaporative emission standards has effectively controlled pollutant emissions, but there will be an increase in unknown reactive species, which also highlights the importance of increasing detection capabilities. Previous studies on the reactivity closure of exhaust gases have shown that with the increasing of emission standards, the proportion of OH reactivity missing increases, and the author infers that these missing reactivity may come from unmeasured OVOCs and L-alkenes, unspecified high oxygen components and semi/intermediate volatile components (Sha et al., 2022). In field observation experiments, it was also found that OVOCs make important contributions to compensation for the missing of OH reactivity (Fuchs et al., 2017). In our research, we also found that compared with the HSL of China V vehicles, the HSL of the China VI vehicles with lower emissions shows more significant OH reactivity missing and higher OVOC emissions, but OVOCs were not the main

596

597598

599

600

601

602

603

604

605

606

607 608

609

610611

612613

614

615

616 617

618

619

620621

622

623





reactivity contributors to evaporative emissions. Compared with the DBL process, HSL shows a higher koH missing, and the high proportion of aromatics implies that another pathway for exploring OH reactivity missing (Lee et al., 2009). Compare with DBL process, Higher temperature of HSL is beneficial for the volatile emissions of large molecular species (such as aromatics) and can also increase the complexity of components. It is important to note that in the study of koh closure analyzed in exhaust and atmospheric environments, the combustion process of fuel and photochemical reactions in the atmosphere can lead to the oxidation of some organic compounds, generating some OVOCs key reactive components. For evaporative emissions, VOCs are derived mainly come from gasoline vapor and vehicle emissions, implying that the direction for the exploration of the reactivity missing of evaporative emissions is different from those for exhaust and atmospheric environments. The number of species directly affects the understanding of k_{OH} closure. As shown in Figure 5e, f and g, using the source profiles provided in the related research, focusing on 35 species, it was found that the missed reactivity would further expand. For China VI vehicles, the average reactivity missing of HSL, DBL24, and DBL48 were 59.3%, 52.2%, and 56.1%, respectively, corresponding to 50.6%, 37.1%, and 41.2% for China V vehicles, respectively. By comparison, the addition of BC-alkenes in this study can further improve the understanding of evaporative emission species, and adding these species can enable some vehicles to achieve reactivity closure. This indicates that BCalkenes were important species in the evaporative emissions of vehicles, and it is necessary to pay attention to this part of the species in the future. Therefore, based on the composition characteristics of reactive chemical components, it can be inferred that L-alkenes, BC-alkenes and aromatics may be important objects to compensate for the missing reactivity. As shown in Figure 7, establishing an evaporative emission VOCs source profiles based on the composition and koh closure characteristics of vehicles (B, C, E and G), and obtain the reactivity contribution of VOCs components in different vehicle models and emission processes. In the calculation of the reactive source profiles for VOCs

625

626

627

628

629

630

631

632

633

634

635

636637

638

639640

641

642643

644

645 646

647

648

649





evaporation emissions, the reactivity weight percentage of each VOCs species was determined based on the reactivity closure feature (i.e., reactivity closure is considered when the missing activity is less than 15%). Among the koh source profiles, 2-methyl-2-butene (8.2 - 22.0%), trans-2-pentene (6.9 - 13.8%), trans-2-butene (4.9 - 18.7%), 2methyl-1-butene (2.9 - 9.1%), m/p-xylene (1.2 - 7.3%) and toluene (1.3 - 4.4%) etc. were the main contributors. Although the concentrations of n-butane, iso-pentane, and n-pentane in the LC-alkanes contributed significantly, their contributions to reactivity were not significant. When a vehicle exhibits high emissions, taking vehicle D as an example, high emission was caused by vehicle aging due to high mileage, resulting in a significant increase in 2-methyl-2-butene (12.7 - 21.2%), 2-methyl-1-butene (6.8 -10.4%), trans-2-pentene (7.4 - 11.9%), trans-2-butene (6.6 - 12.6%), cis-2-butene (3.7 - 6.8%), and iso-pentane (3.4 - 6.0%). When the high emissions of vehicle (The koh test for the DBL48 process of China V vehicle I failed, so the reactivity source profiles composition was not shown here) are caused by abnormal evaporative emission control system (carbon canister), the changes in reactive species will be different from the high emissions of Vehicle D, and the impact of low-carbon species will be more significant. For example, trans-2-butene, cis-2-butene, and n-butane will significantly increase, while the contributions of 2-methyl-2-butene and 2-methyl-1-butene will decrease. This also indicates that when the vehicle's evaporative emission control system is abnormal, the impact of low-carbon alkenes emissions on OH reactivity will be more prominent. Analysis of key reactive species indicates that L-alkenes, and in particular BC-alkenes, are the main contributors to the OH reactivity of evaporative emission sources. This also indicates that in the control of vehicle evaporative emissions, priority can be given to these highly reactive components, and by improving the chemical composition of fuel formula and vehicle emission technology, the reactive impact of evaporative emissions can be reduced.





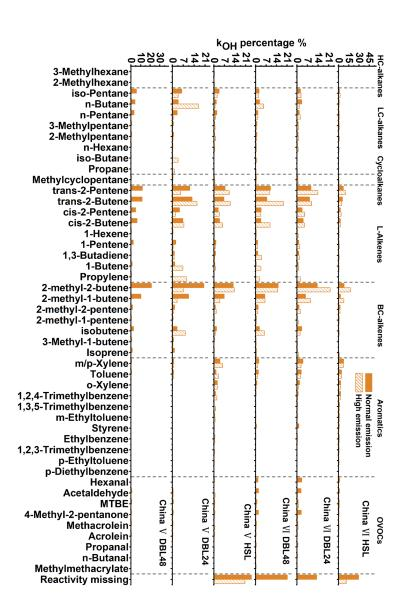


Figure 7. OH reactivity percentage of HSL, DBL24 and DBL48 source profiles for evaporative emissions;

Normal emissions refer to vehicles B, C, E and G; High emissions refer to China VI Vehicle D and China V

Vehicle I.





654

655

656

657

658

659

660

661

662

663

664

665 666

667

668669

670

671

672

673

674 675

676

677

678679

680

681

4. Conclusions

use gasoline vehicles manufactured according to China's current two regulatory standards (China VI and China V) of evaporative emissions. Using improved measurement methods and instruments, the evaporative emission factors, source profiles and OH reactivity characteristics were evaluated. Compared with the China V standard, implementation of the China VI standard can significantly reduce VOCs emissions. During the HSL, DBL24 and DBL48 processes, China V vehicles can reach 3.2, 4.6 and 7.6 times that of China VI vehicles. In the HSL process, aromatics dominate, accounting for 44.1% and 42.8% respectively in China VI and V, followed by LCalkanes at 22.2% and 26.6%, respectively. In the DBL emission process, LC-alkanes dominate, accounting for 40.7% and 42.9% respectively for DBL24 in China VI and V vehicles, and the corresponding proportions were 45.8% and 50.5%, respectively in DBL48. For OVOCs, the proportion of China VI (17.6 - 19.1%) was significantly higher than that of China V (8.5 - 10.1%). For L-alkenes and BC-alkenes, their proportions were 4 - 10.9% and 2.7 - 7.8%, respectively, with China V slightly higher than China VI. Under high evaporative emissions from vehicles, the contribution of LC-alkanes will significantly increase. A source profiles of vehicle evaporative emissions by vehicle models and emission processes were constructed through statistical analysis of the measured species. In the chemical composition, n-butane (3.2 - 26.1%), iso-pentane (6.2 - 13.5%), n-pentane (3.6 - 8.4%), toluene (6.1 - 16.0%), m/p-xylene (2.5 - 10.7%), MTBE (5.3 - 7.4%) and 4-methyl-2-pentanone (0.4 - 5.8%) were the main contributors. For BC-alkenes and Lalkenes, 2-methyl-2-butene (1.6 - 4.3%), 2-methyl-1-butene (0.7 - 2.0%), and trans-2pentene (1.6 - 3.4%) were found to be the main components. The supplementary measurement of BC-alkenes has also expanded the current understanding of the source profiles evaporative emissions from China VI and China V vehicles. In the analysis of evaporative emission tracer ratio, the n-pentane/ethane and MTBE/B ratio serve as a

In this work, we conducted evaporative emission measurements and evaluated of in-





682 diagnostic marker to identify evaporative emissions and other vehicle-related sources. In the koh chemical composition of evaporative emissions, the HSL process was 683 mainly composed of L-alkenes, BC-alkenes and aromatics, accounting for 18.3 - 30.4%, 684 14.8 - 33.4% and 20.9 - 39.8%, respectively. In the DBL process, it was mainly 685 composed of L-alkenes (26.6 - 54.9%) and BC-alkenes (25.7 - 39%). And under high 686 emission conditions, the proportion of L-alkenes and BC-alkenes will increase, 687 indicating that highly reactive species in high emission vehicles have a greater impact. 688 Based on direct measurement and reactivity calculation of koH for closed analysis, it 689 was found that the missing reactivity of China VI was more significant than that of 690 China V vehicles, especially in the HSL process, there are still obvious unknown 691 reactivity sources in China VI (22 - 43.1%) and China V (12.8 - 22.9%). The update of 692 emission standards indicates that the total emissions can be controlled, but there will be 693 an increase in reactive species outside of regulatory monitoring, which hinders the 694 695 comprehensive understanding of air pollution caused by evaporative emission sources. By comparing with literature, it was found that the measurement of BC-alkenes can 696 significantly improve the understanding of the composition of reactive species in 697 698 evaporative emissions. Although n-butane and iso-pentane dominate in emissions, their impact on OH reactivity was not as significant as that of 2-methyl-2-butene, 2-methyl-699 700 1-butene, trans-2-pentene, m/p-xylene and toluene. Therefore, in management VOCs 701 evaporation emissions, a strategy combining total emission reduction with prioritized control of highly reactive species can maximize environmental benefits. 702 703 Author contributions.

- 704 LK and XL design experiments, conceptualize and draft preparation. YW, SH, YL,
- 705 SR and WX analyze data and experimental measurement techniques support. XP, YD,
- 706 YL, MD and SY contributed suggestions, equipment operation, and data analysis. KW,
- 707 FW, XC, JW, YZ and CF contributed measurement technology support. HF, MF, XY,
- 708 LL and YH contributed measuring equipment, measuring techniques, and suggestions.
- 709 **Competing interests.** The authors declare that they have no conflict of interest.
- 710 Financial support. This work was supported by the National Natural Science





- Foundation of China (grant nos. 42277085 and 42477096), and by the Beijing
 Municipal Natural Science Foundation (grant no. JQ21030).
- 713 References
- 714 Chai, J.; Niu, Y.; Yan, Y.; Duan, X.; Zhang, X.; Xing, Y.; Zheng, X.; Peng, L. Variation,
- 715 source and health risk assessment of volatile organic compounds in underground
- 716 park: A case study of an underground park in Beijing, Environmental Chemistry,
- 717 42, 2292-2303, 10.7524/j.issn.0254-6108.2022112203, 2023.
- 718 Chossiere, G. P.; Malin, R.; Allroggen, F.; Eastham, S. D.; Speth, R. L.; Barret, S. R. H.
- 719 Country- and manufacturer-level attribution of air quality impacts due to excess
- NOx emissions from diesel passenger vehicles in Europe, Atmos. Environ., 189,
- 721 89-97, https://doi.org/10.1016/j.atmosenv.2018.06.047, 2018.
- 722 Ministry of Ecology and Environment. China Mobile Source Environmental
- 723 Management Annual Report, 2019.
- 724 Ministry of Ecology and Environment. China Mobile Source Environmental
- 725 Management Annual Report, 2024.
- 726 Fuchs, H.; Tan, Z.; Lu, K.; Bohn, B.; Broch, S.; Brown, S. S.; Dong, H.; Gomm, S.; Häseler,
- 727 R.;He, L.;Hofzumahaus, A.;Holland, F.;Li, X.;Liu, Y.;Lu, S.;Min, K.-E.;Rohrer,
- 728 F.;Shao, M.;Wang, B.;Wang, M.;Wu, Y.;Zeng, L.;Zhang, Y.;Wahner, A.;Zhang, Y.
- 729 OH reactivity at a rural site (Wangdu) in the North China Plain: contributions from
- OH reactants and experimental OH budget, Atmos. Chem. Phys., 17, 654-661,
- 731 https://doi.org/10.5194/acp-17-645-2017, 2017.
- 732 Guan, Y.; Xiao, Y.; Wang, Y.; Zhang, N.; Chu, C. Assessing the health impacts attributable
- 733 to PM_{2.5} and ozone pollution in 338 Chinese cities from 2015 to 2020, Environ.
- 734 Pollut., 287, 117623, https://doi.org/10.1016/j.envpol.2021.117623, 2021.
- 735 Huang, H.; Hu, H.; Zhang, J.; Liu, X. Characteristics of volatile organic compounds from
- vehicle emissions through on-road test in Wuhan, China, Environ. Res., 188,
- 737 109802, https://doi.org/10.1016/j.envres.2020.109802, 2020.
- 738 Huang, J.; Yuan, Z.; Duan, Y.; Liu, D.; Fu, Q.; Liang, G.; Li, F.; Huang, X. Quantification
- 739 of temperature dependence of vehicle evaporative volatile organic compound





- emissions from different fuel types in China, Sci. Total Environ., 813, 152661,
- 741 https://doi.org/10.1016/j.scitotenv.2021.152661, 2022.
- 742 Kovacs, T. A.; Brune, W. H. Total OH Loss Rate Measurement, J. Atmos. Chem., 39,
- 743 105-122, 10.1023/A:1010614113786, 2001.
- 744 Lee, J. D.; Young, J. C.; Read, K. A.; Hamilton, J. F.; Hopkins, J. R.; Lewis, A. C.; Bandy,
- 745 B. J.; Davey, J.; Edwards, P.; Ingham, T.; Self, D. E.; Smith, S. C.; Pilling, M. J.; Heard,
- 746 D. E. Measurement and calculation of OH reactivity at a United Kingdom coastal
- 747 site, J. Atmos. Chem., 64, 53-76, 10.1007/s10874-010-9171-0, 2009.
- 748 Lei, L.; Zhang, Y.; Luo, Y.; Zhang, X.; Feng, M. Analysis of a Typical Ozone Pollution
- Process in the Chengdu Plain Under the Influence of High Temperature Extremes,
- 750 Environ. Sci., 45, 2028-2038, 10.13227/j.hjkx.202305021, 2024.
- 751 Li, C.;Liu, Y.;Cheng, B.;Zhang, Y.;Liu, X.;Qu, Y.;An, J.;Kong, L.;Zhang, Y.;Zhang,
- 752 C.; Tan, Q.; Feng, M. A comprehensive investigation on volatile organic
- 753 compounds (VOCs) in 2018 in Beijing, China: Characteristics, sources and
- behaviours in response to O₃ formation, Sci. Total Environ., 806, 150247,
- 755 https://doi.org/10.1016/j.scitotenv.2021.150247, 2022.
- 756 Li, K.; Jacob, D. J.; Liao, H.; Zhu, J.; Shah, V.; Shen, L.; Bates, K. H.; Zhang, Q.; Zhai, S. A
- 757 two-pollutant strategy for improving ozone and particulate air quality in China,
- 758 Nat. Geosci., 12, 906–910, https://doi.org/10.1038/s41561-019-0464-x, 2019.
- 759 Li, R.; Zhong, C.; Ning, Y.; Liu, Y.; Song, P.; Xu, R.; Mao, H. Exhaust and evaporative
- volatile organic compounds emissions from vehicles fueled with ethanol-blended-
- 761 gasoline, Environ. pollut., 357, 124163,
- 762 https://doi.org/10.1016/j.envpol.2024.124163, 2024.
- 763 Liu, H.; Man, H.; Tschantz, M.; Wu, Y.; He, K.; Hao, J. VOC from Vehicular Evaporation
- 764 Emissions: Status and Control Strategy, Environ. Sci. Technol., 49, 14424-14431,
- 765 https://doi.org/10.1021/acs.est.5b04064, 2015.
- 766 Liu, H.; Man, H.; Cui, H.; Wang, Y.; Deng, F.; Wang, Y.; Yang, X.; Xiao, Q.; Zhang,
- 767 Q.;Ding, Y.;He, K. An updated emission inventory of vehicular VOCs and IVOCs
- 768 in China, Atmos. Chem. Phys., 17, 12709-12724, https://doi.org/10.5194/acp-17-





- 769 12709-2017, 2017.
- 770 Liu, P.; Wu, Y.; Li, Z.; Lv, Z.; Zhang, J.; Liu, Y.; Song, A.; Wang, T.; Wu, L.; Mao, H.; Peng,
- J. Tailpipe volatile organic compounds (VOCs) emissions from Chinese gasoline
- vehicles under different vehicle standards, fuel types, and driving conditions,
- 773 Atmos. Environ., 323, 120348, https://doi.org/10.1016/j.atmosenv.2024.120348,
- 774 2024.
- 775 Liu, S.;Li, X.;Shen, X.;Zeng, L.;Huang, X.;Zhu, B.;Lin, L.;Lou, S. Measurement and
- 776 partition analysis of atmospheric OH reactivity in autumn in Shenzhen, Acta Scien.
- 777 Circum., 39, 3600-3610, 10.13671/j.hjkxxb.2019.0194, 2019.
- 778 Liu, X.; Zhu, R.; Jin, B.; Mei, H.; Zu, L.; Yin, S.; Zhang, R.; Hu, J. Characteristics and
- 779 Source Apportionment of Vehicular VOCs Emissions in a Tunnel Study, Environ.
- 780 Sci., 43, 1777-1787, 10.13227/j.hjke.202108192, 2022a.
- 781 Liu, X.; Yuan, Z.; Sha, Q. e.; Lou, S.; Wang, H.; Li, X.; Zheng, J.; Yuan, B.; Shao, M. Direct
- 782 identification of total and missing OH reactivities from light-duty gasoline vehicle
- exhaust in China based on LP-LIF measurement, J. Environ. Sci., 133, 107-117,
- 784 https://doi.org/10.1016/j.jes.2022.03.041, 2023.
- 785 Liu, Y.; Shao, M.; Fu, L.; Lu, S.; Zeng, L.; Tang, D. Source profiles of volatile organic
- 786 compounds (VOCs) measured in China: Part I, Atmos. Environ., 42, 6247-6260,
- 787 https://doi.org/10.1016/j.atmosenv.2008.01.070, 2008.
- 788 Liu, Y.; Zhong, C.; Peng, J.; Wang, T.; Wu, L.; Chen, Q.; Sun, L.; Sun, S.; Zou, C.; Zhao,
- J.;Song, P.;Tong, H.;Zhang, L.;Wang, W.;Mao, H. Evaporative emission from
- 790 China 5 and China 6 gasoline vehicles: Emission factors, profiles and future
- 791 perspective, J. Cleaner Prod., 331, 129861,
- 792 https://doi.org/10.1016/j.jclepro.2021.129861, 2022b.
- 793 Lou, S.; Holland, F.; Rohrer, F.; Lu, K.; Bohn, B.; Brauers, T.; Chang, C. C.; Fuchs,
- H.;Haeseler, R.;Kita, K.;Kondo, Y.;Li, X.;Shao, M.;Zeng, L.;Wahner, A.;Zhang,
- 795 Y.; Wang, W.; Hofzumahaus, A. Atmospheric OH reactivities in the Pearl River
- 796 Delta China in summer 2006: measurement and model results, Atmos. Chem.
- 797 Phys., 10, 11243-11260, https://doi.org/10.5194/acp-10-11243-2010, 2010.





798 Lu, S.; Bai, Y.; Zhang, G.; Ma, J. Study on the Characteristics of VOCs Source Profiles of Vehicle Exhaust and Gasoline Emission, Acta Sci. Nat. Univ. Pekin., 39, 507-799 511, 10.13209/j.0479-8023.2003.077, 2003. 800 801 Man, H.; Liu, H.; Niu, H.; Wang, K.; Deng, F.; Wang, X.; Xiao, Q.; Hao, J. VOCs evaporative emissions from vehicles in China: Species characteristics of different 802 emission processes, Environ. Sci. Ecotechnol., 100002, 803 1, https://doi.org/10.1016/j.ese.2019.100002, 2020. 804 Man, H.; Liu, H.; Xiao, Q.; Deng, F.; Yu, Q.; Wang, K.; Yang, Z.; Wu, Y.; He, K.; Hao, J. 805 How ethanol and gasoline formula changes evaporative emissions of the vehicles, 806 Appl. Energ., 222, 584-594, https://doi.org/10.1016/j.apenergy.2018.03.109, 2018. 807 Qin, M.; She, Y.; Wang, M.; Wang, H.; Chang, Y.; Tan, Z.; An, J.; Huang, J.; Yuan, Z.; Lu, 808 J.; Wang, Q.; Liu, C.; Liu, Z.; Xie, X.; Li, J.; Liao, H.; Pye, H. O. T.; Huang, C.; Guo, 809 S.;Hu, M.;Zhang, Y.;Jacob, D. J.;Hu, J. Increased urban ozone in heatwaves due 810 811 to temperature-induced emissions of anthropogenic volatile organic compounds, Nat. Geosci., 18, 50-56, https://doi.org/10.1038/s41561-024-01608-w, 2025. 812 813 Rodríguez, F.; Bernard, Y.; Dornoff, J.; Mock, P.: Recommendations for Post-Euro 6 814 Standards for Light-Duty Vehicles in the European Union, The International Council on Clean Transportation Europe, 2019. 815 816 Sha, Q.;Liu, X.;Yuan, Z.;Zheng, J.;Lou, S.;Wang, H.;Li, X.;Yu, F. Upgrading Emission 817 Standards Inadvertently Increased OH Reactivity from Light-Duty Diesel Truck Exhaust in China: Evidence from Direct LP-LIF Measurement, Environ. Sci. 818 Technol., 56, 9968-9977, https://doi.org/10.1021/acs.est.2c02944, 2022. 819 820 Song, M.; Tan, Q.; Feng, M.; Qu, Y.; Liu, X.; An, J.; Zhang, Y. Source Apportionment and Secondary Transformation of Atmospheric Nonmethane Hydrocarbons in 821 Chengdu, Southwest China, J. Geophys. Res-atmos., 123, 9741-9763, 822 https://doi.org/10.1029/2018JD028479, 2018. 823 824 Sun, L.; Liu, Y.; Zhao, J.; Sun, S.; Song, C.; Zhang, J.; Li, Y.; Lin, Y.; Wang, T.; Mao, H. Pollution Characteristics and Emission Factors of VOCs from Vehicle Emissions 825 in the Tianjin Tunnel, Environ. Sci., 40, 104-113, 10.13227/j.hjkx.201804187, 826





827	2019.
828	Wang, H.; Yang, Z.; Jing, S. a. Volatile Organic Compounds (VOCs) Source Profiles of
829	Industrial Processing and Solvent Use Emissions: A Review, Environ. Sci., 38,
830	2617-2628, 10.13227/j.hjkx.201611119, 2017.
831	Wang, R.; Wang, X.; Cheng, S.; Zhu, J.; Zhang, X.; Cheng, L.; Wang, K. Determining an
832	optimal control strategy for anthropogenic VOC emissions in China based on
833	source emissions and reactivity, J. Environ. Sci., 136, 248-260,
834	https://doi.org/10.1016/j.jes.2022.10.034, 2024.
835	Wu, Y.; Yang, Y.; Shao, M.; Lu, S. Missing in total OH reactivity of VOCs from gasoline
836	evaporation, Chin. Chem. Lett., 26, 1246-1248,
837	https://doi.org/10.1016/j.cclet.2015.05.047, 2015.
838	Yan, L.;Zheng, B.;Geng, G.;Hong, C.;Tong, D.;Zhang, Q. Evaporation process
839	dominates vehicular NMVOC emissions in China with enlarged contribution from
840	1990 to 2016, Environ. Res. Lett., 16, 124036, https://doi.org/10.1088/1748-
841	9326/ac3872, 2021.
842	Yang, X.; Wang, H.; Tan, Z.; Lu, K.; Zhang, Y. Observations of OH Radical Reactivity in
843	Field Studies, Acta Chim. Sinica, 77, 613-624, 10.6023/a19030094, 2019.
844	Yue, T.; Yue, X.; Chai, F.; Hu, J.; Lai, Y.; He, L.; Zhu, R. Characteristics of volatile organic
845	compounds (VOCs) from the evaporative emissions of modern passenger cars,
846	Atmos. Environ., 151, 62-69, https://doi.org/10.1016/j.atmosenv.2016.12.008,
847	2017.
848	Yue, T.; Wang, M.; Huang, Z.; Wang, X.; Wang, Z.; Wang, B.; Zhang, L.; Wang, S.
849	Characteristics of Evaporative Emissions from Light-Duty Vehicles and Effects of
850	Ambient Temperature on Evaporative Emissions of Light-Duty Vehicles, Res.
851	Environ. Sci., 33, 73-81, 10.13198/j.issn.1001-6929.2019.07.25, 2020.
852	Zhang, Y.; Wang, X.; Zhang, Z.; Lu, S.; Shao, M.; Lee, F. S. C.; Yu, J. Species profiles and
853	normalized reactivity of volatile organic compounds from gasoline evaporation in
854	China, Atmos. Environ., 79, 110-118,
855	https://doi.org/10.1016/j.atmosenv.2013.06.029, 2013.





856 Zhao, R.; Huang, L.; Zhang, J.; Ooyang, F. Emissions characteristics of volatile organic compounds (VOCs) from typical industries of solvent use in Chengdu City, Acta 857 Scien. Circum., 38, 1147-1154, 10.13671/j.hjkxxb.2017.0362, 2018. 858 Zhong, M.; Tian, J.; Ye, D. China's Total VOCs Control Program Research and 859 Suggestions during the 14th Five-Year Period, Environ. Impact Assess., 43, 1-6, 860 10.14068/j.ceia.2021.02.001, 2021. 861 862 Zhu, Q.;Liu, J.;Zhao, X.;Luo, J. Estimation of light-duty vehicles total evaporative emissions Beijing, China Environ. Sci., 42, 1066-1072, in 863 10.19674/j.cnki.issn1000-6923.2022.0070, 2022. 864 Zhu, R.;Hu, J.;Bao, X.;He, L.;Lai, Y.;Zu, L.;Li, Y.;Su, S. Investigation of tailpipe and 865 evaporative emissions from China IV and Tier 2 passenger vehicles with different 866 **TRANSPORT** RES D-TR E, 50, 305-315, gasolines, 867 https://doi.org/10.1016/j.trd.2016.10.027, 2017. 868 Zi, T.; Wang, P.; Liu, B.; Zhou, Y.; Shen, X. e.; Zhang, L.; Lu, Y.; Feng, Q.; Yang, Y.; Lang, 869 J. Evaporative emission characteristics of VOCs from in-use light-duty gasoline 870 312, 120024, 871 vehicles, Atmos. Environ., https://doi.org/10.1016/j.atmosenv.2023.120024, 2023. 872